

Relaxation dynamics and genuine properties of the solvated electron in neutral water clusters

Thomas E. Gartmann,[¥] Loren Ban,[¥] Bruce L. Yoder, Sebastian Hartweg, Egor Chasovskikh,
and Ruth Signorell*

*Department of Chemistry and Applied Biosciences, Laboratory of Physical Chemistry,
ETH Zürich, Vladimir-Prelog-Weg 2, CH-8093, Zürich, Switzerland*

[¥] These authors contributed equally to this work.

* To whom correspondence should be addressed. E-mail: rsignorell@ethz.ch

Abstract:

We have investigated the solvation dynamics and the genuine binding energy and anisotropy parameter of the solvated electron in neutral water clusters with a combination of time-resolved photoelectron velocity map imaging and electron scattering simulations. The dynamics was probed with a UV probe pulse following above-band-gap excitation with a EUV pump pulse. The solvation dynamics is completed within about 2 ps. Data analysis with an electron scattering model for the ground-state hydrated electron reveals a genuine binding energy in the range of 3.55-3.85 eV and a genuine anisotropy parameter in the range of 0.51-0.66. These genuine cluster values agree well with corresponding experimental and theoretical values for the liquid suggesting similar properties of the solvated electron in liquid water and large neutral water clusters.

INTRODUCTION

The broad attention that solvated electrons in their ground and excited states have attracted over many decades can be attributed to them being among the simplest quantum solutes as well as to their important role in a wide range of fields. Many studies have focused on excess electrons in water and anion water clusters¹⁻³⁶ (and refs. therein). For liquid water, the excited state relaxation dynamics of electrons has been investigated over a broad time window from femtoseconds to beyond picoseconds. This has resulted in the picture of an initially delocalized electron that relaxes to a hydrated electron within ~1 ps; subsequent geminate recombination takes place on a much longer time scale^{11, 16} (and refs. therein). Typically, multi-photon ionization of neat water using different detection schemes has been employed in these investigations. Recent time-resolved photoelectron studies have revealed a non-adiabatic transition from excited electronic states (p-states) to the ground electronic state (s-state) of the hydrated electron on a sub-100 fs timescale followed by slow (several 100 fs) relaxation in the ground electronic state^{9, 10} (and refs. therein). Similarly, the relaxation dynamics often after an s to p excitation was studied as a function of cluster size in photodetachment (anionic cluster) experiments^{12, 14, 15, 31, 35} (and references therein) and in neutral clusters after excitation by an extreme ultraviolet (EUV) light pulse.³⁷

In order to characterize relaxation dynamics and different hydrated electron states, photoelectron studies record the photoelectron kinetic energies and in some cases the photoelectron angular distributions (PAD). Our recent investigation on hydrated electrons in liquid water microjets has, however, revealed that these measurement quantities are strongly influenced by electron transport scattering in the liquid and thus depend on the photon energy of the ionizing laser.³⁶ Typically, experimental electron kinetic energies (eKEs) vary by about 1 eV depending on the energy of the ionizing photon. Furthermore, the experimental PADs of the hydrated electron correspond to an almost isotropic distribution because of electron transport scattering. Proper analysis of the data thus requires that the influence of electron scattering be taken into account.^{36, 38-47} We have shown that corrections by means of a detailed electron scattering model, make it possible to retrieve genuine (intrinsic) values for the electron binding energy (eBE) and the photoelectron angular distribution from experimental data.^{36, 38, 39} These genuine values allow for a meaningful interpretation of the experimental results.

The present study investigates the relaxation dynamics to the ground state solvated electron in large water clusters containing on average ~300 molecules after an above-band-gap excitation by an EUV photon from a high harmonic laser source (pump) and ionization by a UV probe pulse. The major goal is a first characterization of the influence of electron scattering on the measured properties of the ground state hydrated electron in neutral water clusters. We recently found electron scattering cross sections for large water clusters⁴⁸ to be substantially different from the cross sections of condensed (liquid/amorphous solid) phases.^{36, 38, 39} We found that cluster scattering can be treated as an intermediate case between gas⁴⁹ and condensed phase scattering.^{36, 38, 39} The reduced dielectric screening in clusters compared with the condensed phase provides a simple explanation for the increase of the cluster scattering cross sections compared with the condensed phase scattering cross sections.⁴⁸ The present contribution makes a first step towards the retrieval of genuine binding energies and photoemission anisotropies

for neutral water clusters through a combination of experimental data and a detailed scattering model. Such data analysis will be required for future comparisons of the properties of solvated electrons in neutral clusters versus the condensed phase and anion clusters.

EXPERIMENTAL AND SCATTERING SIMULATIONS

The experimental setup used for the measurements in the present work has been described previously.^{48, 50} We used a velocity map imaging (VMI)⁵¹ spectrometer⁵²⁻⁵⁵ to record photoelectron images from water clusters upon photoionization by time-resolved pump and probe laser pulses. EUV light was produced by high harmonic generation (HHG),⁵⁶ as previously described.⁴⁸ A home-built, time-preserving monochromator^{57, 58} was used to select the 7th harmonic (~10.9 eV) which was used as the pump. As a probe pulse, we used 266 nm light generated by frequency tripling of the 800 nm output from the Ti:Sapphire laser. A beam of neutral water clusters was produced and characterized in the same manner as in previous work.⁴⁸ For the experiments presented in this work, the average cluster size was determined to be $\langle n \rangle = 300$ via the sodium-doping method.^{59, 60} See Section S.1 in the Supplementary Information (SI) for details.

The electron scattering simulations have been described previously in detail.^{36, 38, 39, 47, 48} The probabilistic scattering model is based on a Monte Carlo solution of the transport equation. The scattering cross sections, angular dependences, and the energy loss functions of all relevant elastic and inelastic phonon, vibron and electronic scattering channels are explicitly taken into account. Simulations are performed for cluster scattering cross sections (models iii and iv),⁴⁸ liquid water scattering cross sections (model i)⁴⁸ and gas phase scattering cross sections (model ii).⁴⁸ While the scattering cross sections used in models i and iii are taken directly from the previous study,⁴⁸ the cross sections in model ii and iv were adapted to account for the lower electron kinetic energies in the current study. See Section S.2 in the SI for details.

RESULTS

Solvation dynamics:

Figure 1 shows the time evolution of the vertical electron binding energy (VBE), panel a), and the full-width-at-half maximum (FWHM), panel b), of the binding energy spectra recorded after above-band-gap excitation with EUV light of ~10.9 eV photon energy. The VBE increases with time and stabilizes after 1-2 ps at a value of ~3.75 eV, while the FWHM narrows on the same time scale to stabilize at ~1.14 eV (see Section S.3 in the SI with binding energy spectra and fits at different pump-probe delays in Figure S3). The temporal increase in the VBE reflects the formation of a more strongly bound hydrated electron over time. The relaxation time of 1-2 ps is in reasonable agreement with previously reported time-scales for the formation of the ground-state hydrated electron in liquid bulk water and in anionic water clusters^{12, 16, 23, 31, 32, 35} (and references therein). However, one needs to keep in mind that direct comparison with previous studies is difficult because the time scales for equilibration strongly depend on how the electron was initially prepared.³² Analogous to these previous studies, we assume that after

2 ps a hydrated electron in its electronic ground (s-) state has formed in an equilibrated solvent environment. The similarity of the timescales for the total solvation dynamics in liquid water, large anion clusters and large, neutral clusters might not be so surprising at first sight since one of the main processes is the relaxation of the first few solvation shells, which likely occurs on similar time scales in the different systems. However, similar timescales for the solvation dynamics also implies similar localization times of the initially formed delocalized electron for the liquid bulk and neutral clusters. Considering that initial ejection lengths for excitation around ~ 10.9 eV in the liquid are around 3 nm¹¹ and that a cluster size of 300 molecules corresponds to a radius of ~ 1.3 nm, the observed similarity seems less obvious.

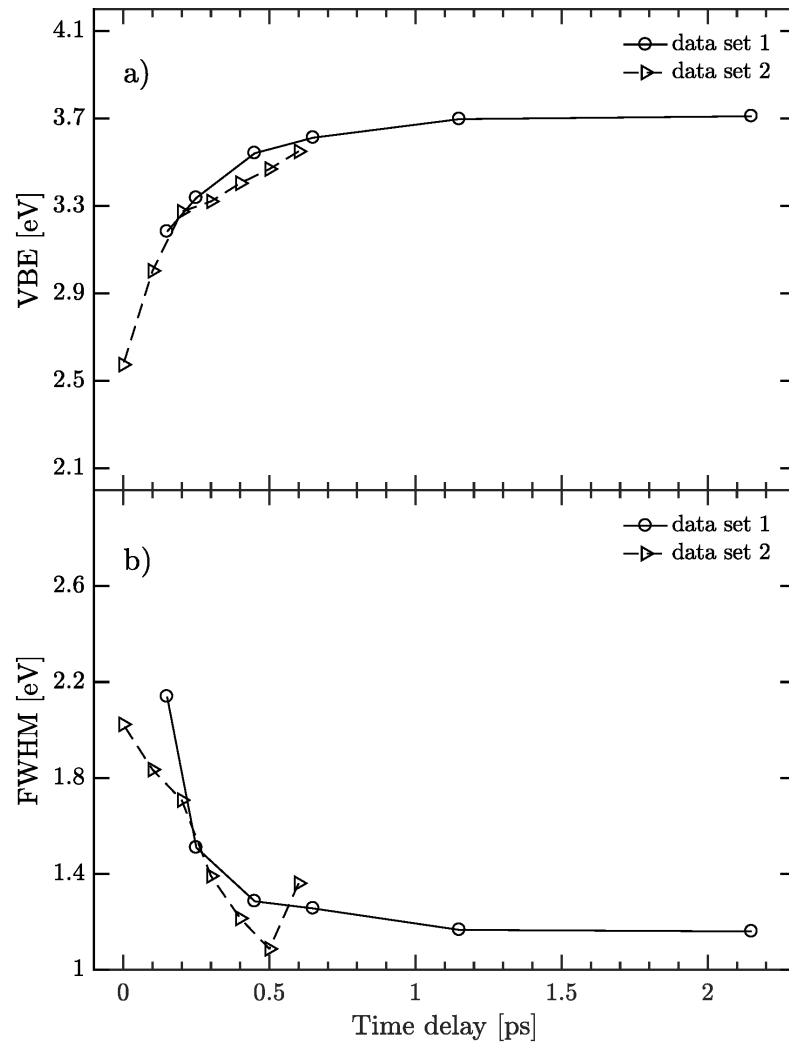


Figure 1. Evolution of the photoelectron signal as a function of the pump-probe time delay. a) Vertical electron binding energy (VBE) and b) full width at half maximum (FWHM). Uncertainties are estimated not to exceed ± 0.2 eV and ± 0.3 eV for VBE and FWHM, respectively. Lines connecting data points are intended as a guide to the eye. Data set 1 and 2 represent independent measurement series providing an impression of the experimental reproducibility.

Genuine properties:

By combining experimental photoelectron VMI images with detailed scattering simulations, we have recently determined genuine vertical binding energies and genuine β -parameters for the ground-state hydrated electron in liquid water.³⁶ Here, we retrieve genuine VBEs (Figure 2) and genuine β -parameters (Figure 3) for the ground-state hydrated electron in large neutral water clusters from the photoelectron VMI images of the clusters recorded after 2 ps (Figure 1). Figure 2a shows the experimental binding energy spectrum at 2 ps time delay together with two simulated spectra. For the calculated, dashed-line spectrum we used the genuine binding energy spectrum of the liquid (see starred spectrum in Figure 3 of Luckhaus et al.³⁶ and dashed-line spectrum in Figure 2b) and the cluster scattering cross sections (model iii) from ref.⁴⁸ for the scattering calculations. The calculated, solid-line spectrum is obtained by fitting a genuine binding energy spectrum (solid line in Figure 2b) to the experimental data using scattering calculations with the same cluster scattering cross sections (model iii in ref.⁴⁸). Contrary to the liquid bulk experiments,³⁶ the experimental cluster data (Figure 2a) are obtained for a single probe energy (266 nm), which is too low to cover the shoulder in the genuine binding energy spectrum of the liquid bulk (dashed-line spectrum in Figure 2b). A single Gaussian is thus sufficient to represent the main part of the genuine binding energy spectrum of the clusters (full line in Figure 2b) covered by the experiment.

Both simulations in Figure 2a represent the experimental spectrum very closely, suggesting that the genuine binding energy spectrum of the hydrated electron in the liquid bulk and in a neutral water cluster with \sim 300 molecules is similar. The same holds for the genuine VBEs listed in Table 1. The liquid value of 3.7 ± 0.1 eV lies in the range of the cluster values of 3.55-3.85 eV, which we determined from a sensitivity analysis using both cluster scattering cross sections (model iii and iv) from ref.⁴⁸ At first glance, this similarity between clusters and liquid might be a bit surprising. However, recent calculations for the VBEs by Herbert and coworkers^{17, 21, 61} have revealed similar VBE values for electrons solvated in the liquid bulk and at the air-liquid interface region (Table 1). These theoretical values agree very well with our cluster values, suggesting similar properties of the hydrated electron in a neutral cluster and the liquid. A distinction as to whether the solvated electron in the clusters resembles more an electron in an interfacial region or rather one in the liquid bulk is not possible based on binding energies alone because they are not specific enough. Assuming cluster-size independent genuine properties, we have simulated the cluster-size dependent influence of electron scattering on the binding energy spectra and VBEs using our cluster scattering model. We found only a minor influence on these experimental observables for clusters in the size range of 100-900 molecules. See Figures S4 in Section S.4 of the SI.

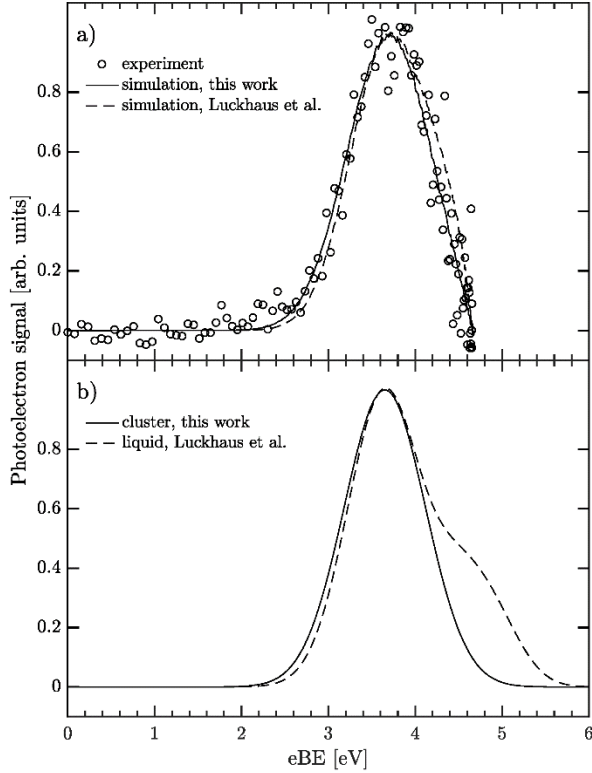


Figure 2. a) Experimental binding energy spectrum recorded at a pump-probe delay of ~ 2 ps (circles). Dashed-line spectrum: Simulation with genuine eBE of the liquid from Luckhaus et al.³⁶ (dashed line in panel b). Full-line spectrum: Simulation with a single Gaussian fit for the cluster genuine eBE (full line in panel b).

Table 1: Values for genuine VBE and genuine β -parameter for the solvated electron in liquid water in the bulk and at the air/water interface region, in neutral water clusters, and in anionic water clusters.

	genuine VBE [eV]	genuine β -parameter
Calc. bulk from refs. ^{17, 21}	3.4-3.6	
Calc. bulk from ref. ⁶¹	3.75 ± 0.55	
Calc. interfacial from refs. ^{17, 21}	3.1-3.2	
Calc. interfacial from ref. ⁶¹	3.35 ± 0.46	
Exp. liquid bulk ³⁶	3.7 ± 0.1	0.6 ± 0.2
Exp. neutral cluster (300 molecules) this work	3.55-3.85	0.51-0.66
Exp. anion cluster ¹⁴ (~ 50 molecules)		$\sim 0.7 \pm 0.1$

A second hint for the similarity of the genuine properties of the hydrated electron in neutral water clusters and in the liquid comes from a comparison of the genuine β -parameters. We have previously determined a genuine β -parameter in the liquid bulk of 0.6 ± 0.2 ,³⁶ which seems in fair agreement with what one would expect for an s-like orbital character of the ground state solvated electron.²¹ For clusters with ~ 300 molecules, we observe an experimental β -parameter of 0.19 ± 0.12 at ~ 2 ps time delay (dashed horizontal line in Figure 3). (Note here that typically, absolute values for β -parameters are not measured to better than ± 0.1 accuracy with VMI setups.) This experimental value, however, is strongly reduced compared with the genuine β -parameter in the cluster due to electron scattering processes. The latter make the genuine photoelectron anisotropy more isotropic, which results in a lowering of the experimental β -parameter. To retrieve the genuine β -parameter in the clusters we have performed scattering simulations, the results of which are shown in Figure 3. The diamonds and the squares show the expected experimental β -parameter as a function of the genuine β -parameter for scattering simulations with the cluster cross sections from model iii and model iv, respectively. This graph reveals that the experimental β -parameter of 0.19 for the clusters is consistent with a genuine β -parameter in the range 0.51-0.66, depending on the cluster scattering cross sections used.⁴⁸ This range of genuine values is again in very good agreement with the genuine value of the liquid (Table 1) and hints that the properties of the ground state electron in the liquid and neutral clusters could indeed be very similar. Not only is this range in fair agreement with the liquid, but also with the value of $\sim 0.7 \pm 0.1$ reported for anionic water clusters containing ~ 50 molecules.¹⁴ The simulations in Figure S5 in the SI provide an idea of the cluster-size dependence of the observable experimental β -parameter predicted as a function of the genuine β -parameter for clusters with 100 to 900 molecules. In contrast to electron binding energy spectra and VBEs (see above), experimental β -parameters are predicted to depend pronouncedly on the cluster size, with systematically lower values for larger clusters as a consequence of the increased number of scattering events in larger clusters.

Figure 3 also shows results for scattering simulations for which we replace the cluster scattering cross sections, either by the scattering cross section of the liquid phase^{36, 38, 39} (circles) or by those of the gas phase⁴⁹ (triangles). For liquid scattering cross sections, our experimental β -parameter of 0.19 would lead to a genuine β -parameter of ~ 0.4 , while for the gas phase scattering cross sections a genuine β -parameter of ~ 1.0 would result. Neither would be fully consistent with the results of the liquid bulk. This further underlines the importance of using proper cross sections to account for the electron transport in a cluster.

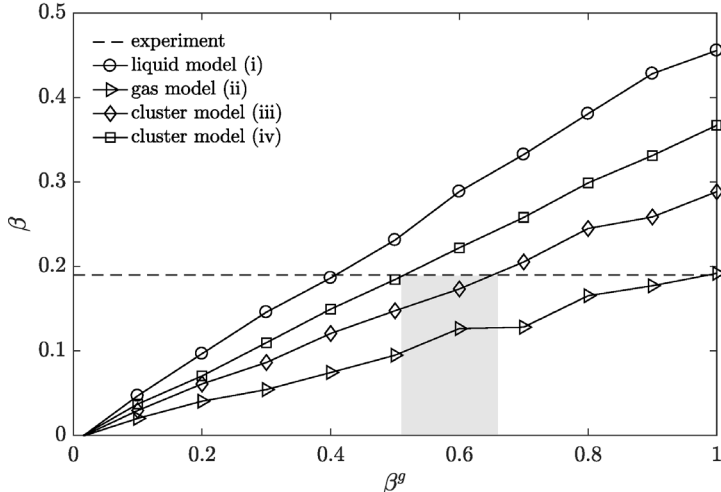


Figure 3. Observable β -values as a function of genuine β -values (β^g) simulated for different models of the electron scattering cross sections (cluster size $\langle n \rangle = 300$; see ref.⁴⁸ for simulation details). Lines in between data points represent linear interpolations. The horizontal dashed line represents the experimental β -value of 0.19. The gray shaded area indicates the range of genuine β -parameters bracketed by cluster models iii and iv, that is consistent with the experimental β -value measured for water clusters.

CONCLUSIONS

We have shown that the formation of the ground-state hydrated electron in neutral water clusters with about 300 molecules after above band-gap excitation is completed within about 2 ps. This time-scale in neutral clusters seems consistent with corresponding dynamics in the liquid water and large anion clusters, hinting at similar mechanisms of the solvation dynamics in the different targets. Likewise, data from photoelectron spectroscopy suggest similar properties for the ground-state solvated electron in large neutral water clusters and liquid water, because the genuine parameters characteristic both for the energetics (VBEs) and for the photoelectron angular distributions (β -parameter) agree for clusters and liquid. Whether the solvated electron in the clusters resembles more an electron in the liquid interfacial region or more one in liquid bulk cannot be decided based on binding energies alone because the latter are likely not specific enough to distinguish between interface and bulk solvated electrons.²¹ It is, however, reasonable to expect similar properties in neutral clusters and in the liquid, since the solvated electron in its ground state appears to be a fairly well localized object strongly interacting with only few neighboring molecules.^{21, 31} A conclusive proof of that presumed similarity in liquid and cluster would require further investigations with other measurement methods probing different (genuine) properties. The direct comparison between different targets (liquid/cluster) and between experiment and theory has only become possible through the determination of genuine parameters, which are no longer influenced by the different degrees of electron scattering in different targets and which do not depend on the probe photon energy used for ionization.³⁶

ACKNOWLEDGEMENTS

We thank David Stapfer and Markus Steger for technical support. This project has received funding from the European Union's Horizon 2020 research and innovation program from the European Research Council under the Grant Agreement No 786636, and was supported by the NCCR MUST, funded by the Swiss National Science Foundation (SNSF), through ETH-FAST, and through SNSF project no. 200020_172472.

REFERENCES

- (1) Yamamoto, Y.-I.; Suzuki, Y.-I.; Tomasello, G.; Horio, T.; Karashima, S.; Mitrić, R.; Suzuki, T. Time- and Angle-Resolved Photoemission Spectroscopy of Hydrated Electrons near a Liquid Water Surface. *Phys. Rev. Lett.* **2014**, *112*, 187603.
- (2) Yamamoto, Y.; Karashima, S.; Adachi, S.; Suzuki, T. Wavelength Dependence of Uv Photoemission from Solvated Electrons in Bulk Water, Methanol, and Ethanol. *J. Phys. Chem. A* **2016**, *120*, 1153-1159.
- (3) Horio, T.; Shen, H.; Adachi, S.; Suzuki, T. Photoelectron Spectra of Solvated Electrons in Bulk Water, Methanol, and Ethanol. *Chem. Phys. Lett.* **2012**, *535*, 12-16.
- (4) Faubel, M.; Siefermann, K. R.; Liu, Y.; Abel, B. Ultrafast Soft X-Ray Photoelectron Spectroscopy at Liquid Water Microjets. *Acc. Chem. Res.* **2012**, *45*, 120-130.
- (5) Siefermann, K. R.; Liu, Y.; Lugovoy, E.; Link, O.; Faubel, M.; Buck, U.; Winter, B.; Abel, B. Binding Energies, Lifetimes and Implications of Bulk and Interface Solvated Electrons in Water. *Nature Chem.* **2010**, *2*, 274-279.
- (6) Lübcke, A.; Buchner, F.; Heine, N.; Hertel, I. V.; Schultz, T. Time-Resolved Photoelectron Spectroscopy of Solvated Electrons in Aqueous NaI Solution. *Phys. Chem. Chem. Phys.* **2010**, *12*, 14629-14634.
- (7) Buchner, F.; Schultz, T.; Lübcke, A. Solvated Electrons at the Water-Air Interface: Surface Versus Bulk Signal in Low Kinetic Energy Photoelectron Spectroscopy. *Phys. Chem. Chem. Phys.* **2012**, *14*, 5837-5842.
- (8) Shreve, A. T.; Elkins, M. H.; Neumark, D. M. Photoelectron Spectroscopy of Solvated Electrons in Alcohol and Acetonitrile Microjets. *Chem. Sci.* **2013**, *4*, 1633-1639.
- (9) Elkins, M. H.; Williams, H. L.; Shreve, A. T.; Neumark, D. M. Relaxation Mechanism of the Hydrated Electron. *Science* **2013**, *342*, 1496-1499.
- (10) Karashima, S.; Yamamoto, Y.; Suzuki, T. Resolving Nonadiabatic Dynamics of Hydrated Electrons Using Ultrafast Photoemission Anisotropy. *Phys. Rev. Lett.* **2016**, *116*, 137601.
- (11) Elles, C. G.; Jialaubekov, A. E.; Crowell, R. A.; Bradforth, S. E. Excitation-Energy Dependence of the Mechanism for Two-Photon Ionization of Liquid H₂O and D₂O from 8.3 to 12.4 eV. *J. Chem. Phys.* **2006**, *125*, 044515.
- (12) Young, R. M.; Neumark, D. M. Dynamics of Solvated Electrons in Clusters. *Chem. Rev.* **2012**, *112*, 5553-5577.

(13) Chen, X.; Bradforth, S. E. The Ultrafast Dynamics of Photodetachment. *Annu. Rev. Phys. Chem.* **2008**, *59*, 203-231.

(14) Bragg, A. E.; Verlet, J. R. R.; Kammerath, A.; Cheshnovsky, O.; Neumark, D. M. Electronic Relaxation Dynamics of Water Cluster Anions. *J. Am. Chem. Soc.* **2005**, *127*, 15283-15295.

(15) Griffin, G. B.; Young, R. M.; Ehrler, O. T.; Neumark, D. M. Electronic Relaxation Dynamics in Large Anionic Water Clusters: $(\text{H}_2\text{O})_N^-$ and $(\text{D}_2\text{O})_N^-$ (N=25–200). *J. Chem. Phys.* **2009**, *131*, 194302.

(16) Savolainen, J.; Uhlig, F.; Ahmed, S.; Hamm, P.; Jungwirth, P. Direct Observation of the Collapse of the Delocalized Excess Electron in Water. *Nature Chem.* **2014**, *6*, 697-701.

(17) Coons, M. P.; You, Z. Q.; Herbert, J. M. The Hydrated Electron at the Surface of Neat Liquid Water Appears to Be Indistinguishable from the Bulk Species. *J. Am. Chem. Soc.* **2016**, *138*, 10879-10886.

(18) Uhlig, F.; Marsalek, O.; Jungwirth, P. Electron at the Surface of Water: Dehydrated or Not? *J. Phys. Chem. Lett.* **2013**, *4*, 338-343.

(19) Casey, J. R.; Schwartz, B. J.; Glover, W. J. Free Energies of Cavity and Noncavity Hydrated Electrons near the Instantaneous Air/Water Interface. *J. Phys. Chem. Lett.* **2016**, *7*, 3192-3198.

(20) Borgis, D.; Rossky, P. J.; Turi, L. Electronic Excited State Lifetimes of Anionic Water Clusters: Dependence on Charge Solvation Motif. *J. Phys. Chem. Lett.* **2017**, *8*, 2304-2309.

(21) Herbert, J. M.; Coons, M. P. The Hydrated Electron. *Annu. Rev. Phys. Chem.* **2017**, *68*, 447-472.

(22) Stähler, J.; Deinert, J. C.; Wegkamp, D.; Hagen, S.; Wolf, M. Real-Time Measurement of the Vertical Binding Energy During the Birth of a Solvated Electron. *J. Am. Chem. Soc.* **2015**, *137*, 3520-3524.

(23) Sagar, D. M.; Bain, C. D.; Verlet, J. R. R. Hydrated Electrons at the Water/Air Interface. *J. Am. Chem. Soc.* **2010**, *132*, 6917-6919.

(24) Nowakowski, P. J.; Woods, D. A.; Verlet, J. R. R. Charge Transfer to Solvent Dynamics at the Ambient Water/Air Interface. *J. Phys. Chem. Lett.* **2016**, *7*, 4079-4085.

(25) Elkins, M. H.; Williams, H. L.; Neumark, D. M. Isotope Effect on Hydrated Electron Relaxation Dynamics Studied with Time-Resolved Liquid Jet Photoelectron Spectroscopy. *J. Chem. Phys.* **2016**, *144*, 184503.

(26) Riley, J. W.; Wang, B. X.; Woodhouse, J. L.; Assmann, M.; Worth, G. A.; Fielding, H. H. Unravelling the Role of an Aqueous Environment on the Electronic Structure and Ionization of Phenol Using Photoelectron Spectroscopy. *J. Phys. Chem. Lett.* **2018**, *9*, 678-682.

(27) Coe, J. V.; Arnold, S. T.; Eaton, J. G.; Lee, G. H.; Bowen, K. H. Photoelectron Spectra of Hydrated Electron Clusters: Fitting Line Shapes and Grouping Isomers. *J. Chem. Phys.* **2006**, *125*, 014315.

(28) Ma, L.; Majer, K.; Chirot, F.; von Issendorff, B. Low Temperature Photoelectron Spectra of Water Cluster Anions. *J. Chem. Phys.* **2009**, *131*, 144303.

(29) Ehrler, O. T.; Neumark, D. M. Dynamics of Electron Solvation in Molecular Clusters. *Acc. Chem. Res.* **2009**, *42*, 769-777.

(30) Lietard, A.; Verlet, J. R. R. Selectivity in Electron Attachment to Water Clusters. *J. Phys. Chem. Lett.* **2019**, *10*, 1180-1184.

(31) Turi, L.; Rossky, P. J. Theoretical Studies of Spectroscopy and Dynamics of Hydrated Electrons. *Chem. Rev.* **2012**, *112*, 5641-5674.

(32) Kambhampati, P.; Son, D. H.; Kee, T. W.; Barbara, P. F. Solvation Dynamics of the Hydrated Electron Depends on Its Initial Degree of Electron Delocalization. *J. Phys. Chem. A* **2002**, *106*, 2374-2378.

(33) Lian, R.; Oulianov, D. A.; Shkrob, I. A.; Crowell, R. A. Geminate Recombination of Electrons Generated by above-the-Gap (12.4 eV) Photoionization of Liquid Water. *Chem. Phys. Lett.* **2004**, *398*, 102-106.

(34) Kratz, S.; Torres-Alacan, J.; Urbanek, J.; Lindner, J.; Vöhringer, P. Geminate Recombination of Hydrated Electrons in Liquid-to-Supercritical Water Studied by Ultrafast Time-Resolved Spectroscopy. *Phys. Chem. Chem. Phys.* **2010**, *12*, 12169-12176.

(35) Paik, D. H.; Lee, I.-R.; Yang, D.-S.; Baskin, J. S.; Zewail, A. H. Electrons in Finite-Sized Water Cavities: Hydration Dynamics Observed in Real Time. *Science* **2004**, *306*, 672-675.

(36) Luckhaus, D.; Yamamoto, Y. I.; Suzuki, T.; Signorell, R. Genuine Binding Energy of the Hydrated Electron. *Sci. Adv.* **2017**, *3*, e1603224.

(37) LaForge, A. C.; Michiels, R.; Bohlen, M.; Callegari, C.; Clark, A.; von Conta, A.; Coreno, M.; Di Fraia, M.; Drabbels, M.; Huppert, M.; et al. Real-Time Dynamics of the Formation of Hydrated Electrons Upon Irradiation of Water Clusters with Extreme Ultraviolet Light. *Phys. Rev. Lett.* **2019**, *122*, 133001.

(38) Signorell, R.; Goldmann, M.; Yoder, B. L.; Bodi, A.; Chasovskikh, E.; Lang, L.; Luckhaus, D. Nanofocusing, Shadowing, and Electron Mean Free Path in the Photoemission from Aerosol Droplets. *Chem. Phys. Lett.* **2016**, *658*, 1-6.

(39) Michaud, M.; Wen, A.; Sanche, L. Cross Sections for Low-Energy (1-100 eV) Electron Elastic and Inelastic Scattering in Amorphous Ice. *Radiat. Res.* **2003**, *159*, 3-22.

(40) Ottosson, N.; Faubel, M.; Bradforth, S. E.; Jungwirth, P.; Winter, B. Photoelectron Spectroscopy of Liquid Water and Aqueous Solution: Electron Effective Attenuation Lengths and Emission-Angle Anisotropy. *J. Electron Spectrosc. Relat. Phenom.* **2010**, *177*, 60-70.

(41) Thürmer, S.; Seidel, R.; Faubel, M.; Eberhardt, W.; Hemminger, J. C.; Bradforth, S. E.; Winter, B. Photoelectron Angular Distributions from Liquid Water: Effects of Electron Scattering. *Phys. Rev. Lett.* **2013**, *111*, 173005.

(42) Suzuki, Y.-I.; Nishizawa, K.; Kurahashi, N.; Suzuki, T. Effective Attenuation Length of an Electron in Liquid Water between 10 and 600 eV. *Phys. Rev. E* **2014**, *90*, 010302.

(43) Shinotsuka, H.; Da, B.; Tanuma, S.; Yoshikawa, H.; Powell, C. J.; Penn, D. R. Calculations of Electron Inelastic Mean Free Paths. XI. Data for Liquid Water for Energies from 50 eV to 30 keV. *Surf. Interface Anal.* **2017**, *49*, 238-252.

(44) Olivieri, G.; Parry, K. M.; Powell, C. J.; Tobias, D. J.; Brown, M. A. Quantitative Interpretation of Molecular Dynamics Simulations for X-Ray Photoelectron Spectroscopy of Aqueous Solutions. *J. Chem. Phys.* **2016**, *144*, 154704.

(45) Zhang, C.; Andersson, T.; Förstel, M.; Mucke, M.; Arion, T.; Tchaplyguine, M.; Björneholm, O.; Hergenhahn, U. The Photoelectron Angular Distribution of Water Clusters. *J. Chem. Phys.* **2013**, *138*, 234306.

(46) Nishitani, J.; West, C. W.; Suzuki, T. Angle-Resolved Photoemission Spectroscopy of Liquid Water at 29.5 eV. *Struct. Dyn.* **2017**, *4*, 044014.

(47) Hartweg, S.; Yoder, B. L.; Garcia, G. A.; Nahon, L.; Signorell, R. Size-Resolved Photoelectron Anisotropy of Gas Phase Water Clusters and Predictions for Liquid Water. *Phys. Rev. Lett.* **2017**, *118*, 103402.

(48) Gartmann, T. E.; Hartweg, S.; Ban, L.; Chasovskikh, E.; Yoder, B. L.; Signorell, R. Electron Scattering in Large Water Clusters from Photoelectron Imaging with High Harmonic Radiation. *Phys. Chem. Chem. Phys.* **2018**, *20*, 16364-16371.

(49) Itikawa, Y.; Mason, N. Cross Sections for Electron Collisions with Water Molecules. *J. Phys. Chem. Ref. Data* **2005**, *34*, 1-22.

(50) Gartmann, T. E.; Yoder, B. L.; Chasovskikh, E.; Signorell, R. Lifetimes and Energetics of the First Electronically Excited States of NaH₂O from Time-Resolved Photoelectron Imaging. *Chem. Phys. Lett.* **2017**, *683*, 515-520.

(51) Eppink, A.; Parker, D. H. Velocity Map Imaging of Ions and Electrons Using Electrostatic Lenses: Application in Photoelectron and Photofragment Ion Imaging of Molecular Oxygen. *Rev. Sci. Instrum.* **1997**, *68*, 3477-3484.

(52) Yoder, B. L.; West, A. H. C.; Schläppi, B.; Chasovskikh, E.; Signorell, R. A Velocity Map Imaging Photoelectron Spectrometer for the Study of Ultrafine Aerosols with a Table-Top VUV Laser and Na-Doping for Particle Sizing Applied to Dimethyl Ether Condensation. *J. Chem. Phys.* **2013**, *138*, 044202.

(53) West, A. H. C.; Yoder, B. L.; Signorell, R. Size-Dependent Velocity Map Photoelectron Imaging of Nanosized Ammonia Aerosol Particles. *J. Phys. Chem. A* **2013**, *117*, 13326-13335.

(54) Signorell, R.; Yoder, B. L.; West, A. H. C.; Ferreiro, J. J.; Saak, C.-M. Angle-Resolved Valence Shell Photoelectron Spectroscopy of Neutral Nanosized Molecular Aggregates. *Chem. Sci.* **2014**, *5*, 1283-1295.

(55) West, A. H. C.; Yoder, B. L.; Luckhaus, D.; Signorell, R. Solvated Electrons in Clusters: Magic Numbers for the Photoelectron Anisotropy. *J. Phys. Chem. A* **2015**, *119*, 12376-12382.

(56) Ferray, M.; L'Huillier, A.; Li, X. F.; Lompre, L. A.; Mainfray, G.; Manus, C. Multiple-Harmonic Conversion of 1064 nm Radiation in Rare Gases. *Journal of Physics B: Atomic, Molecular and Optical Physics* **1988**, *21*, L31-L35.

(57) Frassetto, F.; Cacho, C.; Froud, C. A.; Turcu, I. C. E.; Villoresi, P.; Bryan, W. A.; Springate, E.; Poletto, L. Single-Grating Monochromator for Extreme-Ultraviolet Ultrashort Pulses. *Optics Express* **2011**, *19*, 19169-19181.

(58) Frassetto, F.; Miotti, P.; Poletto, L. Grating Configurations for the Spectral Selection of Coherent Ultrashort Pulses in the Extreme-Ultraviolet. *Photonics* **2014**, *1*, 442-454.

(59) Bobbert, C.; Schütte, S.; Steinbach, C.; Buck, U. Fragmentation and Reliable Size Distributions of Large Ammonia and Water Clusters. *Eur. Phys. J. D* **2002**, *19*, 183-192.

- (60) Yoder, B. L.; Litman, J. H.; Forysinski, P. W.; Corbett, J. L.; Signorell, R. Sizer for Neutral Weakly Bound Ultrafine Aerosol Particles Based on Sodium Doping and Mass Spectrometric Detection. *J. Phys. Chem. Lett.* **2011**, 2, 2623-2628.
- (61) Coons, M. P.; Herbert, J. M. Quantum Chemistry in Arbitrary Dielectric Environments: Theory and Implementation of Nonequilibrium Poisson Boundary Conditions and Application to Compute Vertical Ionization Energies at the Air/Water Interface. *J. Chem. Phys.* **2018**, 148, 222834.

Supporting Information:

**Relaxation dynamics and genuine properties of the solvated electron
in neutral water clusters**

Thomas E. Gartmann, [¥] Loren Ban, [¥] Bruce L. Yoder, Sebastian Hartweg, Egor Chasovskikh,
and Ruth Signorell

Department of Chemistry and Applied Biosciences, Laboratory of Physical Chemistry,

ETH Zürich, Vladimir-Prelog-Weg 2, CH-8093, Zürich, Switzerland

[¥] These authors contributed equally to this work.

S.1. Size determination of the neutral cluster distribution:

Figure S1 shows a neutral size distribution of water clusters used in this work. The average cluster size, $\langle n \rangle$, was determined to be 300 water molecules via the sodium-doping method¹⁻³ with analysis as described in detail previously.⁴ Panel a) shows a typical mass spectrum of the neutral water cluster size distribution as recorded with the Na-doping method. The resulting cluster abundances are shown in panel b) after all relevant corrections were applied.

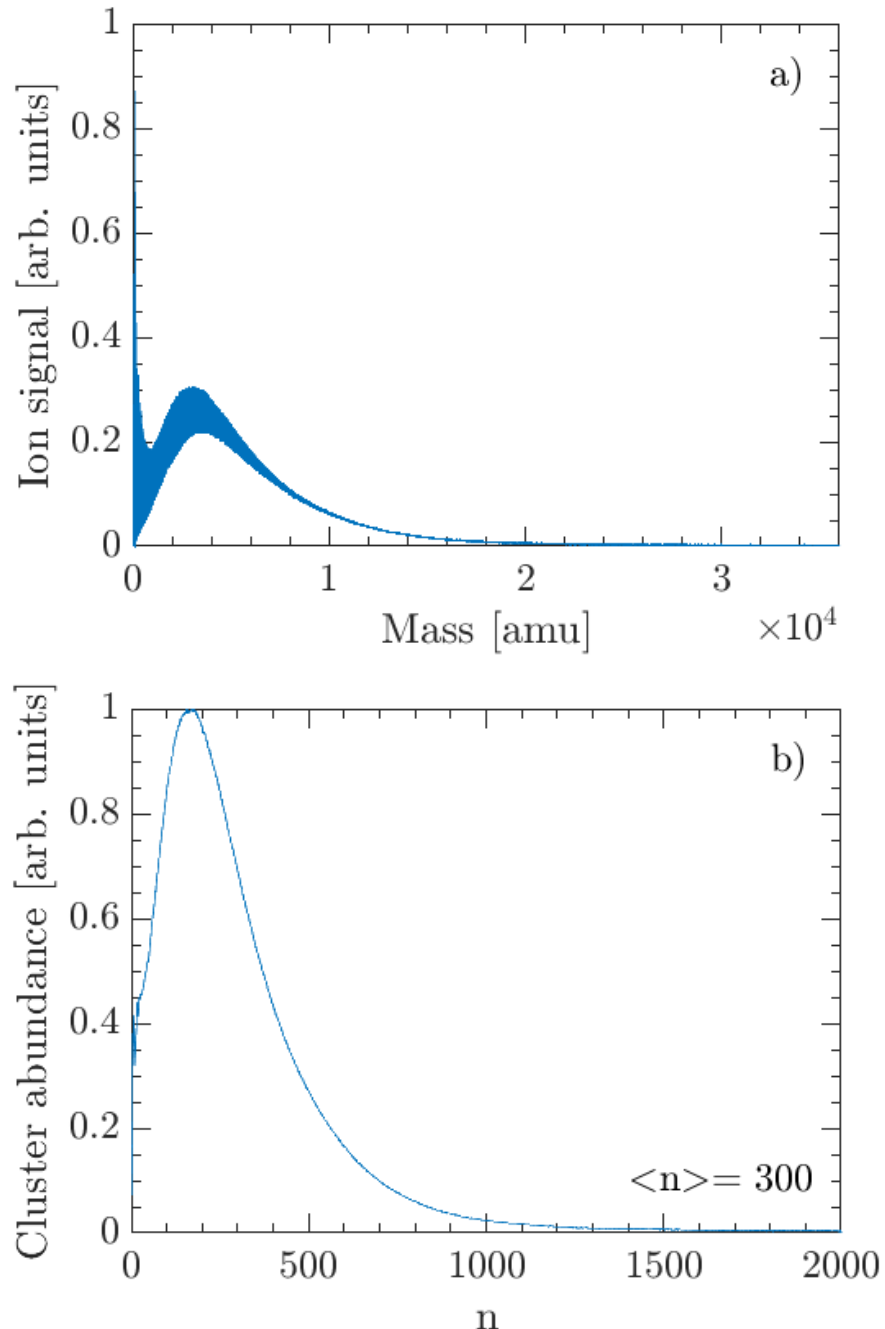


Figure S1: a) Typical mass spectrum for cluster size determination, recorded with the Na-doping method. b) Corresponding neutral cluster size distribution with $\langle n \rangle = 300$.

S.2. Determination of electron scattering cross sections for clusters:

To mimic gas phase electron scattering (Figure S2, model (ii), dashed red lines) the liquid bulk scattering cross sections of model (i) were scaled with constant factors to match the corresponding gas phase data recommended by Itikawa and Mason⁶ (green circles and green line). The scaling factors for quasi-elastic and vibrational scattering channels are 8 and 7 respectively. Note that electronic scattering channels do not contribute in the energy range below 5 eV kinetic energy for which these scaling factors are determined. The scaling factors used in this study differ from the ones previously determined⁴ due to the different electron kinetic energy range considered. The procedure itself however, is identical to previous work.⁴ For the quasi-elastic processes (Figure S2 a)), the sum of the liquid bulk elastic scattering cross sections and the isotropic parts of all liquid bulk phonon related scattering cross sections was scaled to match the gas phase momentum transfer cross sections given by Itikawa and Mason.⁶ For the vibrational scattering processes (Figure S2 b)) their sum was compared with the sum of all gas phase vibrational cross sections.⁶ In order to sum the vibrational scattering cross sections for the gas phase, the data given by Itikawa and Mason was first linearly interpolated.

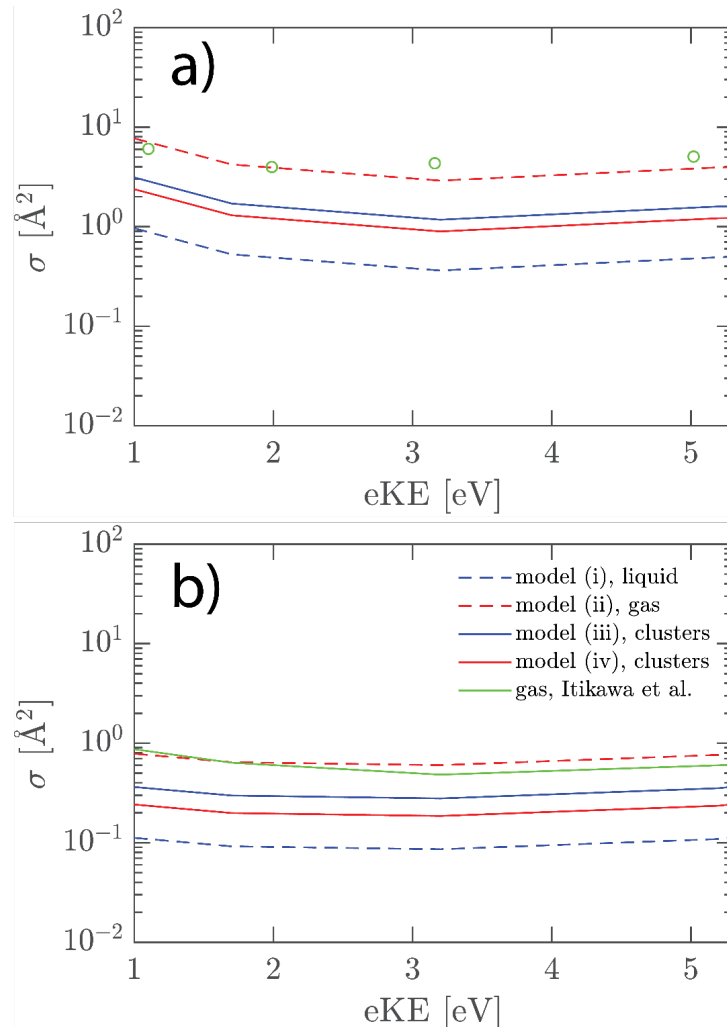


Figure S2: Total electron scattering cross sections for quasi-elastic (a) and vibrational scattering (b) in liquid water (blue dashed lines), gas phase water (red dashed lines) and clusters (blue and red full lines). Gas phase scattering cross sections derived from Itikawa and Mason⁶ are shown as green circles and full green lines.

To obtain scattering cross sections that reproduce the situation in the clusters (model (iii) and model (iv)) the liquid and the gas phase scattering cross sections are scaled with the square of the dielectric constant at optical frequencies ($1.8^2=3.24$). This scaling factor is used to multiply the scattering cross sections of the liquid bulk (model (i)) to describe a situation without dielectric screening (model (iii)), as an intermediate case between the gas phase and the liquid phase. A second intermediate case (model (iv)) is created by dividing the gas phase scattering cross sections (model (ii)) by 3.24. Both models ((iii) and (iv)) have been shown to qualitatively describe electron scattering in neutral water clusters with < 1000 molecules.⁴

S.3. VMI data analysis:

Recorded velocity map images were reconstructed using MEVELER⁵ resulting in photoelectron kinetic energy and angular distributions, described with a single anisotropy parameter β

$$I(\theta) \propto 1 + \frac{\beta}{2}(3 \cos^2 \theta - 1),$$

where $I(\theta)$ is the signal at angle θ defined between the laser polarization vector and the ejection direction of the photoelectrons. Photoelectron spectra were fitted using a single Gaussian function to extract the vertical binding energies (VBEs) and full widths at half maximum (FWHMs) as a function of the pump-probe delay (Figure S3). The fit was performed for the data points in the eBE region below ~ 4.1 eV. The photoelectron anisotropy parameter β was subsequently determined as an average over the half width at half maximum obtained from the fit.

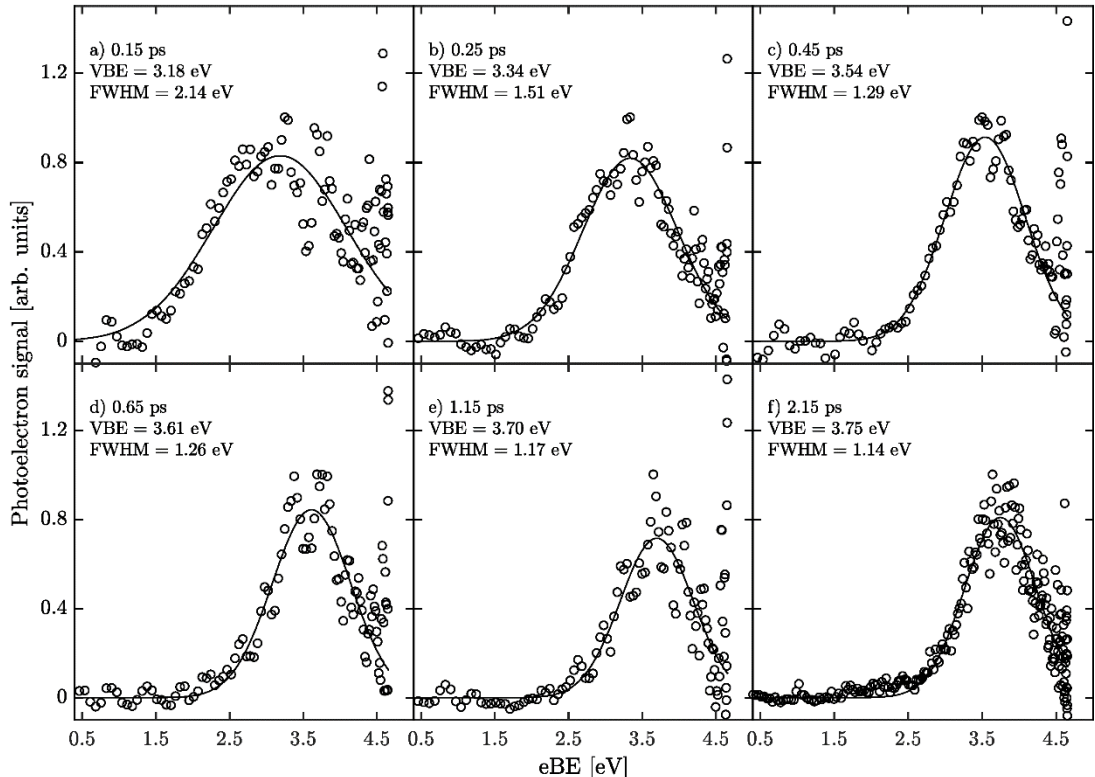


Figure S3: Time-dependent photoelectron spectra and corresponding Gaussian fits used to determine VBEs and FWHMs. Spectra for delays < 2 ps have been smoothed by a 3 point moving average.

S.4. Size-dependence of the VBE and the β -parameter:

Figure S4 shows simulated photoelectron spectra as a function of cluster size given in number of water molecules, n . Genuine values determined from the fit to the experimental results (Figure 2 in the main text) were used in the simulation. It is clear that the cluster size has a very minor influence on the kinetic energy spectra in the range $n=100-900$ water molecules. In contrast, the effect of size is more pronounced for the β -parameter (Figure S5).

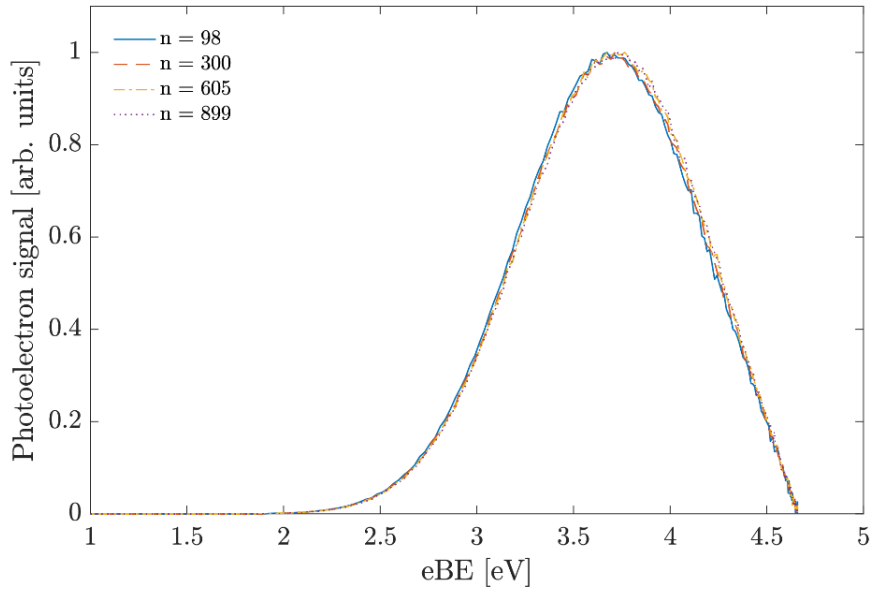


Figure S4: Size-dependence of the simulated photoelectron spectra.

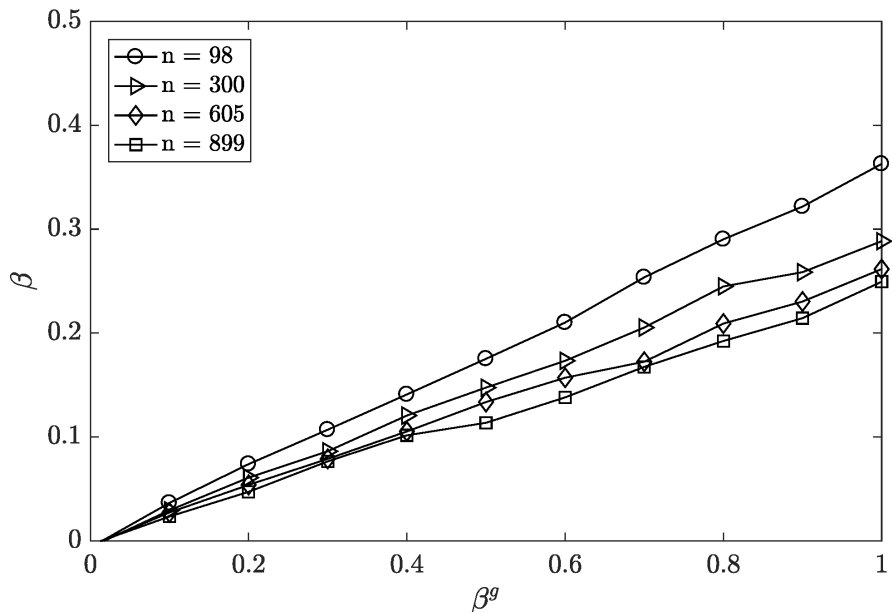


Figure S5: Size-dependence of the observable β value as a function of the genuine β -parameter (β^g).

REFERENCES

- (1) Bobbert, C.; Schütte, S.; Steinbach, C.; Buck, U. Fragmentation and Reliable Size Distributions of Large Ammonia and Water Clusters. *Eur. Phys. J. D* **2002**, *19*, 183-192.
- (2) Yoder, B. L.; Litman, J. H.; Forysinski, P. W.; Corbett, J. L.; Signorell, R. Sizer for Neutral Weakly Bound Ultrafine Aerosol Particles Based on Sodium Doping and Mass Spectrometric Detection. *J. Phys. Chem. Lett.* **2011**, *2*, 2623-2628.
- (3) Litman, J. H.; Yoder, B. L.; Schläppi, B.; Signorell, R. Sodium-Doping as a Reference to Study the Influence of Intracluster Chemistry on the Fragmentation of Weakly-Bound Clusters Upon Vacuum Ultraviolet Photoionization. *Phys. Chem. Chem. Phys.* **2013**, *15*, 940-949.
- (4) Gartmann, T. E.; Hartweg, S.; Ban, L.; Chasovskikh, E.; Yoder, B. L.; Signorell, R. Electron Scattering in Large Water Clusters from Photoelectron Imaging with High Harmonic Radiation. *Phys. Chem. Chem. Phys.* **2018**, *20*, 16364-16371.
- (5) Dick, B. Inverting Ion Images without Abel Inversion: Maximum Entropy Reconstruction of Velocity Maps. *Phys. Chem. Chem. Phys.* **2014**, *16*, 570-580.
- (6) Itikawa, Y.; Mason, N. Cross Sections for Electron Collisions with Water Molecules. *J. Phys. Chem. Ref. Data* **2005**, *34*, 1-22.